J. Plasma Physics (2007), *vol.* 73, *part* 3, *pp.* 403–415. © 2006 Cambridge University Press
doi:10.1017/S0022377806004636 First published online 3 July 2006 Printed in the United Kingdom

Electrostatic solitary structures in a charge-varying pair–ion–dust plasma

MOULOUD TRIBECHE, LEILA AIT GOUGAM, NADIA BOUBAKOUR and TAHA HOUSSINE ZERGUINI

Faculty of Sciences-Physics, Theoretical Physics Laboratory, University of Bab-Ezzouar, USTHB, B.P. 32, El Alia, Algiers 16111, Algeria

(Received 12 March 2006)

Abstract. Large-amplitude electrostatic solitary structures are investigated in an unmagnetized charge-varying pair–ion–dust plasma in which electrons and positrons have equal masses. Their spatial patterns are significantly modified by the presence of the positron component. In particular, it may be noted that an addition of a small concentration of positrons abruptly reduces the potential pulse amplitude as well as the net negative charge residing on the dust grain surface. Under certain conditions, the solitary wave suffers the well-known anomalous damping leading to the development of collisionless shock waves. This investigation may be taken as a prerequisite for the understanding of the electrostatic solitary waves that may occur in space dusty plasmas.

1. Introduction

Recently, low-temperature plasmas containing, in addition to electrons and ions, finite-sized highly charged particulate matter have been studied by many authors because of the frequent occurrence of such plasmas in laboratory, space, and astrophysical plasma environments, such as cometary tails, asteroid zones, planetary rings, interstellar medium, and the Earth's ionosphere and magnetosphere [1–7]. Besides these, dust particles have been observed in low-temperature laboratory discharges including processing plasmas in the semiconductor industry and plasma crystal. While the importance of such interest cannot be overemphasized, in recent years there has been phenomenal growth in research activities in this area as highlighted in recent reviews [4, 8, 9]. Because of the high charge and large mass of the grain particulates compared with those of ions, new time and space scales come into play, giving rise to new wave instabilities in the dusty plasmas. It has been found both theoretically and experimentally that the presence of static charged dust grains modifies the existing plasma wave spectra. On the other hand, it has been shown that the dust charge dynamics introduces new eigenmodes, such as the dust-acoustic (DA) mode [10], the dust ion-acoustic (DIA) mode [11], the dust Bernstein–Greene–Kruskal (DBGK) modes [12], etc. The most well studied of such modes is the so-called 'dust acoustic wave' (DAW), which arises owing to the restoring force provided by the plasma thermal pressure (electrons and ions) while the inertia is due to the dust mass. One of the most interesting types of nonlinear waves is the solitary wave. The soliton results from the balance of two effects, which are the necessary ingredients to obtain a soliton solution for a

https://doi.org/10.1017/S0022377806004636 Published online by Cambridge University Press

nonlinear wave: nonlinearity gives rise to a process that leads to the well-known wave-steepening phenomena. The wave steepening, if not stopped by some other physical phenomena, leads to wave breaking. The plasma dispersion prevents the wave breaking, which is thereby stopped. Solitons of large amplitude have been studied extensively in recent years [13–28]. The analysis have been derived on the basis of the Sagdeev quasipotentials or the reductive perturbation theory, which leads to the dynamical system being described by the Korteweg–de Vries or derivative nonlinear Schrödinger type equations.

In the past, there has been a great deal of interest in understanding different types of collective processes in electron–positron–ion plasmas [29–48]. It is well known that when positrons are introduced into an electron–ion plasma the response of the latter changes significantly. In contrast to the usual two component plasma, it has been observed that the nonlinear waves in plasmas having an additional positron component behave differently [49]. Such pair (electrons and positrons)–ion plasmas are common in supernovae, pulsar environments, cluster explosions, active galactic nuclei, etc. Recently, several authors have discussed the linear as well as the nonlinear properties of pair–ion plasmas containing heavy charged dust grains. Shukla et al. [50] investigated the nonlinear propagation of low-frequency electrostatic waves in a strongly magnetized electron–positron plasma in the presence of parallel [50] and perpendicular [51] sheared plasma flows and massive charged dust grains. Cho et al. [52] investigated the dispersion properties of electromagnetic surface waves in a magnetized dusty electron–positron plasma. Shukla and Marklund [53] demonstrated the existence of dust acoustic waves in strongly magnetized electron–positron–dust plasmas. Shin and Jung [54] investigated the pair annihilation effects on the dust ion acoustic surface wave in semi-bounded magnetized electron–positron–ion–dust plasmas.

The aim of the present paper is therefore to present a theoretical model to show the existence and formation of large-amplitude electrostatic solitary potentials in a charge-varying pair–ion–dust plasma in which electrons and positrons have equal masses. The grain charge becomes a new self-consistent dynamical variable and represents an additional degree of freedom. We emphasis here that for the description of such solitary waves we use the model [55] that enabled us to describe nonlinear DBGK modes. The manuscript is organized as follows. In the next section, we present the basic equations of our model. Our numerical results are presented and discussed in Sec. 3. A summary of our results is given in Sec. 4.

2. Theoretical model

Let us consider an unmagnetized dusty plasma having electrons, positrons, ions, and dust grains of density n_e, n_p, n_i, and n_d, respectively. We assume for simplicity that all the grains have the same charge, equal to $q_d = -eZ$, with Z positive for negatively charged dust and negative for positively charged dust. All the dust grains are assumed to have the same size and to be spheres of radius r. Following [12], let us consider the time-independent Vlasov equation with spatial variation only in the $\widehat{x}$-direction,

$$\left(v_x \frac{\partial}{\partial x} - \frac{q_s}{m_s}\frac{d\phi}{dx}\frac{\partial}{\partial v_x}\right) f_s(x, v_x) = 0. \tag{1}$$

https://doi.org/10.1017/S0022377806004636 Published online by Cambridge University Press

Here q_s, m_s, and f_s represent the charge, mass and distribution function of a particle of species s. Poisson's equation is used to determine self-consistently the electrostatic potential $\phi(x)$ in terms of the equilibrium distribution functions of the three species that exist in the plasma,

$$\frac{\partial^2\phi}{\partial x^2} = -4\pi \sum_{s=\mathrm{e,i,p,d}} q_s \int_{-\infty}^{+\infty} dv_x\, f_s(x, v_x), \tag{2}$$

where it is understood that the v_y and v_z dependencies of $f_s(x, v_x)$ have been integrated over. We already know the solutions of (1). Since the electron, ion, positron, and dust distributions can be arbitrarily chosen, subject only to the condition (in one dimension) that

$$f_s(x, v_x) = f_s(E_s) \tag{3}$$

in the wave frame, we can pick three arbitrary functions, one for each species, insert these in (2), and solve the resulting equation. The total energy E_s of a particle of species s is given by

$$E_{s=\mathrm{e,i,p}} = \tfrac{1}{2} m_s v_x^2 + q_s \phi(x). \tag{4}$$

Since the dust grain charge is allowed to change, E_d is rewritten as [55]

$$E_\mathrm{d} = \frac{1}{2} m_\mathrm{d} v_x^2 + \int_0^\phi q_\mathrm{d}\, d\phi \tag{5}$$

so that E_d becomes a constant of the motion and thus $f(E_\mathrm{d})$ satisfies the stationary Vlasov equation. Let us begin to study (2) by looking at a simple case, where each species is a cold beam of particles, each particle of species s having the same speed at a given position. Thus, we choose

$$f_{\alpha=\mathrm{e,i,p}}(x, v_x) = n_{\alpha 0} \frac{v_{\alpha 0}}{\tilde{v}_\alpha} \delta(v_x - \tilde{v}_\alpha)$$

$$f_\mathrm{d}(x, v_x) = n_{\mathrm{d}0} \frac{v_{\mathrm{d}0}}{\tilde{v}_\mathrm{d}} \delta(v_x - \tilde{v}_\mathrm{d}) \tag{6}$$

where

$$\tilde{v}_{\alpha=\mathrm{e,i,p}} = \left(v_{\alpha 0}^2 - \frac{2q_\alpha}{m_\alpha} \phi(x) \right)^{1/2}$$

$$\tilde{v}_\mathrm{d} = \left(v_{\mathrm{d}0}^2 - \frac{2}{m_\mathrm{d}} \int_0^\phi q_\alpha\, d\phi \right)^{1/2} \tag{7}$$

and $\alpha = \mathrm{e, i, p, d}$ refer to electrons, ions, positrons, and variable charge dust grains. Here, $v_{\mathrm{e}0}$, $v_{\mathrm{p}0}$, $v_{\mathrm{i}0}$, and $v_{\mathrm{d}0}$ are chosen large enough so that (7) always yields real positive values for $\tilde{v}_\mathrm{e}$, $\tilde{v}_\mathrm{i}$, $\tilde{v}_\mathrm{p}$, and $\tilde{v}_\mathrm{d}$. Integrating f_e, f_i, f_p and f_d over all velocity space, we find

$$N_\alpha(x) = \frac{n_\alpha(x)}{n_{\alpha 0}} = \frac{v_{\alpha 0}}{\tilde{v}_\alpha} \tag{8}$$

so that (2) becomes

$$\frac{d^2\Psi}{dX^2} = \frac{2/f_1}{\sqrt{1+\alpha_1\Psi}} - \frac{2}{\sqrt{1-\Psi}} - \frac{2f_2/f_1}{\sqrt{1-\alpha_2\Psi}} + \frac{2(f_1+f_2-1)}{f_1} \frac{Z}{Z_0} \frac{1}{\sqrt{1+\beta\xi}} \tag{9}$$

where

$$f_1 = n_{\mathrm{i}0}/n_{\mathrm{e}0}, \quad f_2 = n_{\mathrm{p}0}/n_{\mathrm{e}0}, \quad \alpha_1 = W_\mathrm{i}/W_\mathrm{e}, \quad \alpha_2 = W_\mathrm{i}/W_\mathrm{p}, \quad \beta = W_\mathrm{i}/W_\mathrm{d} \tag{10}$$

https://doi.org/10.1017/S0022377806004636 Published online by Cambridge University Press

and

$$\xi = \int_0^{\Psi} Z\, d\Psi. \tag{11}$$

The normalized quantities

$$\Psi = 2\frac{e\phi}{W_{\rm i}}, \quad X = \frac{\omega_{\rm i}}{v_{\rm i0}}x \tag{12}$$

are introduced and $\omega_{\rm i} = (4\pi n_{\rm i0}e^2/m_{\rm i})^{1/2}$ is an effective ion plasma frequency. $W_\alpha = m_\alpha v_{\alpha 0}^2$ is twice the particle unperturbed kinetic energy. Charge neutrality at equilibrium requires

$$Z_0 n_{\rm d0}/n_{\rm p0} + 1 = f_1 + f_2. \tag{13}$$

Dust grains become charged owing to different processes, such as collection of charged particles from the surrounding plasma, photoionization, secondary electron emission, sputtering by energetic ions, etc. For simplicity, we assume that the collection of charged particles is the prevailing charging process although other charging mechanisms such as photo-, thermal-, or secondary electron emission can substantially affect the dust charging in realistic cases. In the standard probe model for the dust grain, the latter is charged by the plasma currents at the grain surface [56–61]. The charging current originates from electrons, positrons, and ions hitting the grain surface. Typically, the net effect of these currents is to negatively charge the dust grains in equilibrium. The variable dust charge $q_{\rm d} = -eZ$ is determined self-consistently by (note that we consider a one-dimensional stationary plasma)

$$\begin{aligned}\tilde{v}_{\rm d}\frac{\partial q_{\rm d}}{\partial x} &= I_{\rm e} + I_{\rm i} + I_{\rm p}\\ &= -e\int_{v_{\min}}^{\infty} f_{\rm e}(x,v_x)v_x\sigma_{\rm e}(v_x,q_{\rm d})\,dv_x + e\int_0^{\infty} f_{\rm i}(x,v_x)v_x\sigma_{\rm i}(v_x,q_{\rm d})\,dv_x\\ &\quad + e\int_0^{\infty} f_{\rm p}(x,v_x)v_x\sigma_{\rm p}(v_x,q_{\rm d})\,dv_x\end{aligned} \tag{14}$$

which describes charge conservation. $I_{\rm e}$, $I_{\rm p}$, and $I_{\rm i}$ are the average microscopic electron, positron, and ion currents entering the dust grains, as governed by the potential difference between the grain surface and the local plasma. They are obtained by averaging the effective collision cross section $\sigma_{\rm e,p,i}$ for charged particles impacting the dust grains over the electron, positron, and ion distribution functions. $v_{\min} = (-2eq_{\rm d}/m_{\rm e}C)^{1/2}$ is the minimum speed an electron must have in order to arrive at the grain surface. $C = r(1 + r/r_{\rm De}) \simeq r$ is the effective grain capacitance, r the dust grain radius, and $r_{\rm De}$ the electron Debye length. After performing the integrals in (14) and rearranging the terms, one can obtain the following normalized equation,

$$\begin{aligned}\frac{dZ}{dX} = \frac{\pi r^2 n_{\rm e0}v_{\rm e0}v_{\rm i0}}{\omega_{\rm i}v_{\rm d0}}\frac{1}{[1+\beta\xi]^{1/2}}\Bigg\{&\left(1 - \frac{2e^2}{rW_{\rm e}}\frac{Z}{1+\alpha_1\Psi}\right)\\ &- f_1\sqrt{\alpha_1\frac{m_{\rm e}}{m_{\rm i}}}\left(1 + \frac{2e^2}{rW_{\rm i}}\frac{Z}{1-\Psi}\right) - f_2\sqrt{\frac{\alpha_1}{\alpha_2}}\left(1 + \frac{2e^2}{rW_{\rm p}}\frac{Z}{1-\alpha_2\Psi}\right)\Bigg\}\end{aligned} \tag{15}$$

provided that $v_{\min} \prec \tilde{v}_{\rm e}$ (this constraint originates from (14) after performing the plasma electron current integral). Equation (15) is the additional dynamical equation that is coupled to the plasma equations through the plasma currents. The

https://doi.org/10.1017/S0022377806004636 Published online by Cambridge University Press

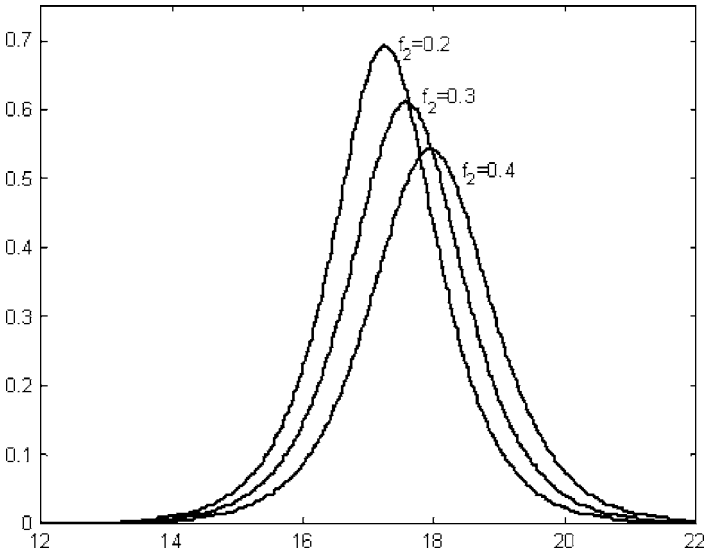


Figure 1. Soliton solution for the electrostatic potential Ψ for various values of f_2 with $Z_0 = 10$, $f_1 = 3$, $r = 3$ μm, $\alpha_1 = 4$, $\alpha_2 = 1$, $\beta = 1/50$, and $n_{d0} = 10^5$ cm^{-3}. The values of v_{i0} deduced from (16) are $v_{i0} = 3.01 \times 10^5$ cm s^{-1} ($f_2 = 0.2$), $v_{i0} = 4.09 \times 10^5$ cm s^{-1} (0.3), and $v_{i0} = 8.69 \times 10^5$ cm s^{-1} ($f_2 = 0.4$). The values of f_2 are indicated on the figure.

dust electric charge becomes a dynamical variable that is coupled self-consistently to the other dynamical variables such as the particle densities and the electrostatic potential. Initially, in the absence of any perturbation ($\Psi = 0$), (15) yields

$$W_i = \frac{2e^2 Z_0}{r} \frac{\alpha_1 + f_1\sqrt{\alpha_1 m_e/m_i} + f_2\sqrt{\alpha_1\alpha_2}}{1 - f_1\sqrt{\alpha_1 m_e/m_i} - f_2\sqrt{\alpha_1/\alpha_2}}. \tag{16}$$

It may be useful to note that (16) does not represent the condition for balancing the plasma currents that determines the floating potential. In the following numerical simulation, the value of W_i is deduced from the above relation while the other remaining parameters are given first.

3. Numerical results

We now proceed with the presentation of our numerical results. One can numerically solve the system of equations (9), (11), and (15) either as a boundary-value problem or as an initial-value problem. For simplicity, we have solved it as an initial-value problem. Equations (9), (11), and (15) are then integrated numerically using a Runge–Kutta scheme suitable for stiff problems and assuming a hydrogen plasma with dust grains of mass density $\rho = 3$ g cm^{-3}. To start the numerical integration, a small edge ($X = 0$) electric field $E_0 = -(d\Psi/dX) = -10^{-11}$ is assumed. It is worth noting that one can take some other values of $(d\Psi/dX)$: an increase (decrease) in its value only shifts the potential or density profile towards (away from) the origin. For the sake of comparison, we have plotted the results for various values of f_2 in Fig. 1. The electrostatic potential Ψ exhibits a spatially localized (soliton-like) structure. The parameters $Z_0 = 10$, $f_1 = 3$, $r = 3$ μm, $\alpha_1 = 4$, $\alpha_2 = 1$, $\beta = 1/50$, and $n_{d0} = 10^5$ cm^{-3} have been chosen so that the conditions for the existence of soliton solutions are fulfilled. Any vanishingly small initial disturbance E_0 will

https://doi.org/10.1017/S0022377806004636 Published online by Cambridge University Press

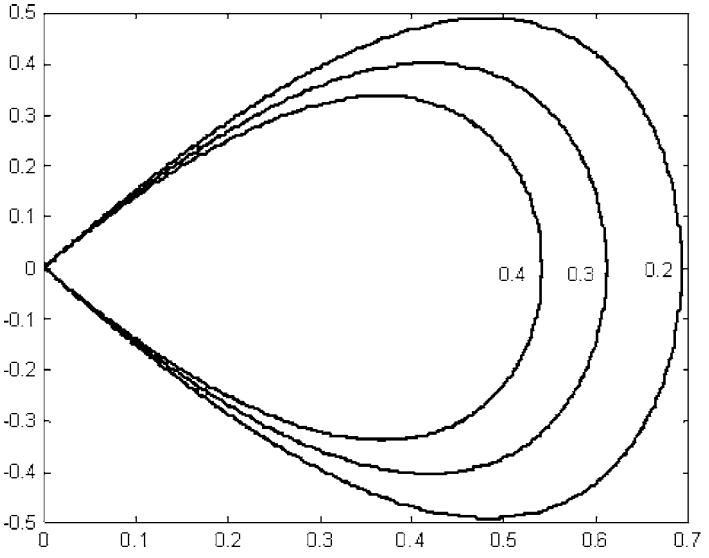


Figure 2. Phase plane trajectories $(d\Psi/dX, \Psi)$. The values of the relevant parameters are those used for Fig. 1. The values of f_2 are indicated on the figure.

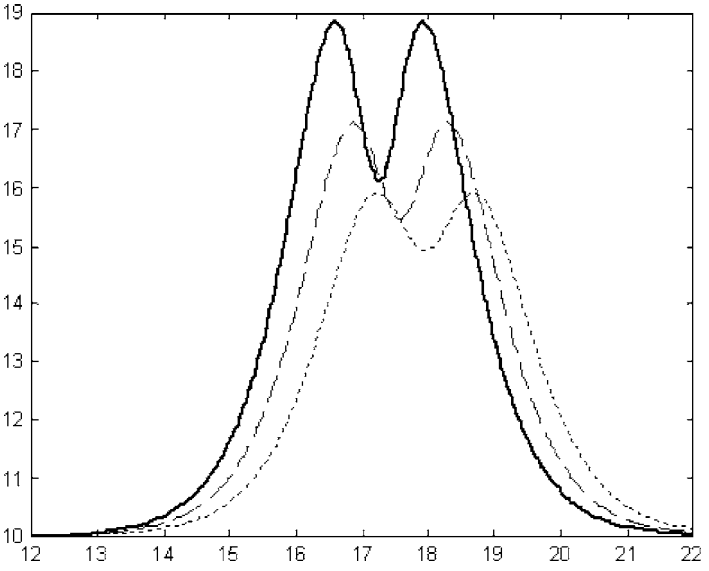


Figure 3. Spatial profile of the dust grain charge Z for various values of $f_2 = 0.2$ (full curve), 0.3 (dashed curve), and 0.4 (dotted curve). The values of the relevant parameters are those used for Fig. 1.

develop into a highly localized nonlinear structure. The results reveal that the spatial patterns of the electrostatic solitary wave are significantly modified by the presence of positrons. With an increase of the parameter $f_2 = n_{p0}/n_{e0}$, the pulse amplitude decreases and the addition of a small concentration of positrons ($f \sim 0.45$) can even prevent soliton formation. This behavior of Ψ can be best understood by plotting phase plane trajectories $(d\Psi/dX, \Psi)$. Each separatrice shown in Fig. 2 represents a bounded localized structure. The dust charge adopts a double-humped

https://doi.org/10.1017/S0022377806004636 Published online by Cambridge University Press

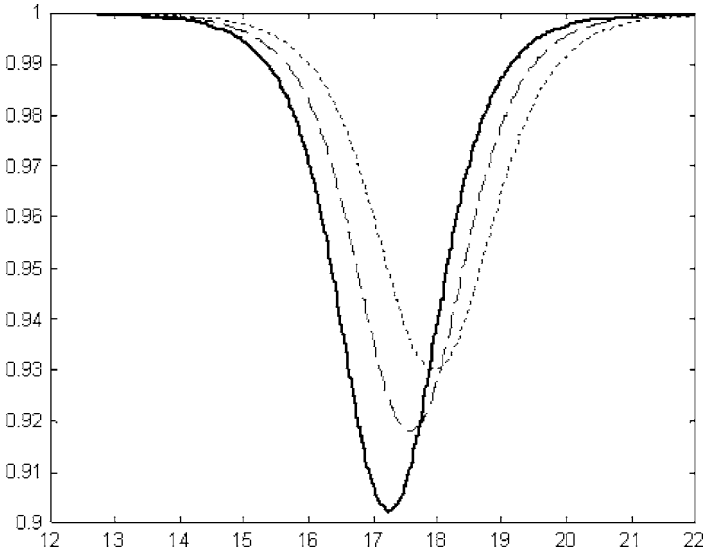


Figure 4. Spatial profile of the dust number density N_d for various values of $f_2 = 0.2$ (full curve), 0.3 (dashed curve), and 0.4 (dotted curve). The values of the relevant parameters are those used for Fig. 1.

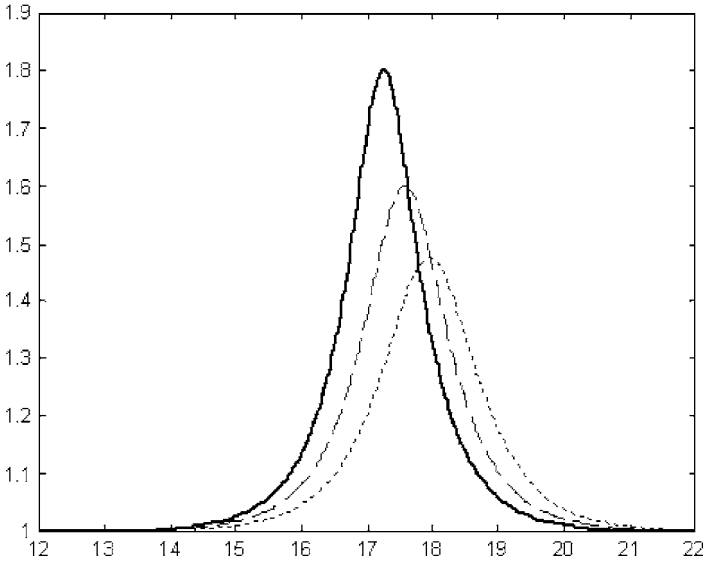


Figure 5. Spatial profile of the positron number density N_p for various values of $f_2 = 0.2$ (full curve), 0.3 (dashed curve), and 0.4 (dotted curve). The values of the relevant parameters are those used for Fig. 1.

solitary profile and remains negative (Fig. 3). It is seen that an addition of minute quantities of positrons abruptly reduces the net negative charge of the dust grain. In fact, as n_{p0} increases, the dust grain collects more positrons, therefore reducing the net negative charge residing on the dust grain surface (the dust grain charge becomes least negative). The dust particle density N_d is given in Fig. 4. The dust particles are locally expelled and pushed out of the region of the soliton's

https://doi.org/10.1017/S0022377806004636 Published online by Cambridge University Press

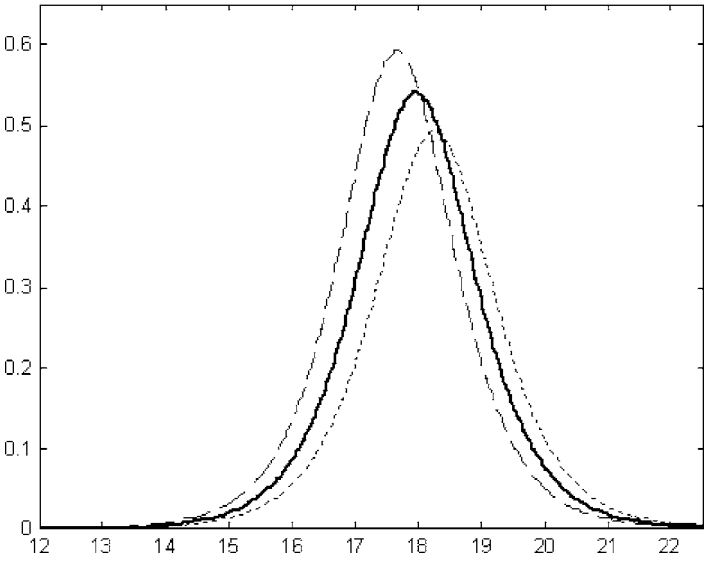


Figure 6. Soliton solution for the eletrostatic potential Ψ versus X for various values of $\alpha_2 = 0.9$ (dashed curve), 1 (full curve), and 1.1 (dotted curve). The remaining parameters are those used for Fig. 1 with $f_2 = 0.4$. The values of v_{i0} deduced from (16) are $v_{i0} = 1.64 \times 10^6$ cm s^{-1} ($\alpha_2 = 0.9$), $v_{i0} = 8.69 \times 10^5$ cm s^{-1} ($\alpha_2 = 1$), and $v_{i0} = 6.85 \times 10^5$ cm s^{-1} ($\alpha_2 = 1.1$).

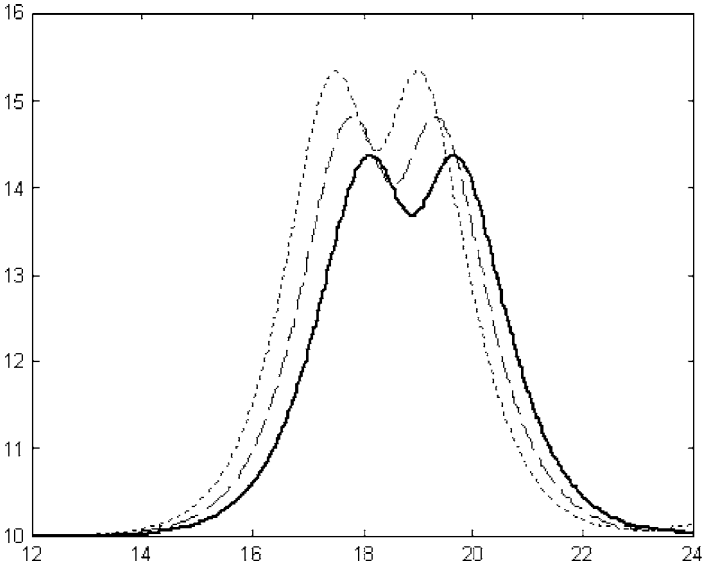


Figure 7. Spatial profile of the dust grain charge Z for various values of $\alpha_2 = 1.1$ (dotted curve), 1.2 (dashed curve), and 1.3 (full curve). The values of the remaining parameters are those used for Fig. 6. The values of v_{i0} deduced from (16) are $v_{i0} = 6.85 \times 10^5$ cm s^{-1} ($\alpha_2 = 1.1$), $v_{i0} = 5.96 \times 10^5$ cm s^{-1} ($\alpha_2 = 1.2$), and $v_{i0} = 5.41 \times 10^5$ cm s^{-1} ($\alpha_2 = 1.3$).

https://doi.org/10.1017/S0022377806004636 Published online by Cambridge University Press

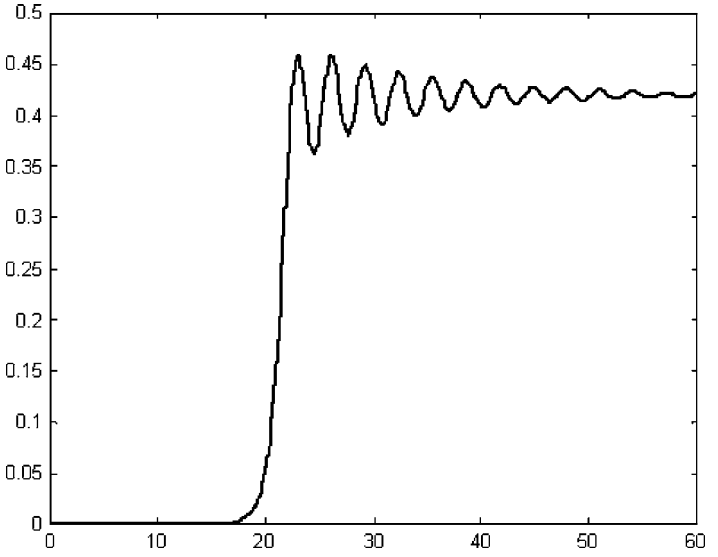


Figure 8. Shock-like solution for the electrostatic potential Ψ with $Z_0 = 50$, $f_1 = 3$, $f_2 = 0.2$, $r = 0.1$ μm, $\alpha_1 = 5$, $\alpha_2 = 1$, $\beta = 1/50$ ($v_{d0} = 360.07$ cm s^{-1}), and $n_{d0} = 10^5$ cm^{-3}. The values of v_{i0} deduced from (16) are $v_{i0} = 4.41 \times 10^6$ cm s^{-1}.

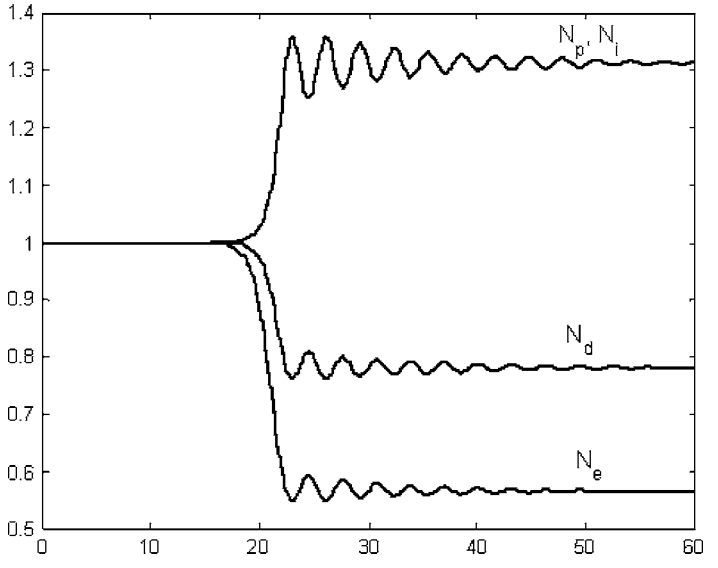


Figure 9. Spatial profile of the electron, positron, ion, and dust densities. The values of the relevant parameters are those used for Fig. 8.

localization, a phenomena which can generate an intense and spiky electric field in the medium. This dust depletion is caused by a balance of the electrostatic forces on the grains and contributes to the positive electrostatic potential field. Note that an increase of f_2 would lead to a decrease of the depth as well as the width of the localized dust void (hole): the dust void shrinks (enlarges) when f_2 is decreased. These nonlinear localized structures (holes) are self-consistent solutions

https://doi.org/10.1017/S0022377806004636 Published online by Cambridge University Press

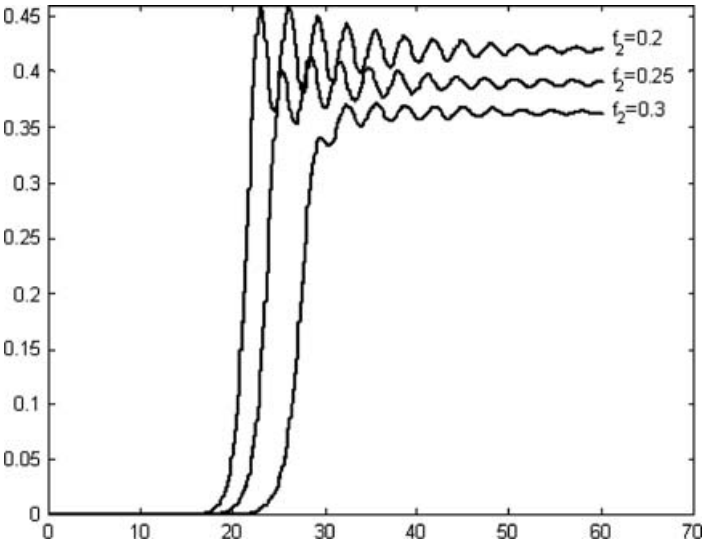


Figure 10. Shock-like solution for the electrostatic potential Ψ for various values of f_2. The values of v_{i0} deduced from (16) are $v_{i0} = 4.41 \times 10^6$ cm s^{-1} ($f_2 = 0.2$), $v_{i0} = 5.26 \times 10^6$ cm s^{-1} (0.25), and $v_{i0} = 6.81 \times 10^6$ cm s^{-1} ($f_2 = 0.3$). The values of f_2 are indicated on the figure. The values of the remaining parameters are those used for Fig. 8.

of the Vlasov equation representing saturated states of a four-stream unstable collisionless dusty plasma. The saturation is provided by an interplay between the nonlinearities (principally due to particle trapping) and dust charge variation. Note that an increase (decrease) of f_2 would lead to a weak (strong) localization of the positrons (Fig. 5). In Fig. 6, we show the spatial patterns of the electrostatic potential Ψ for different values of $\alpha_2 = W_i/W_p$, which exhibits a localized solitary structure. As α_2 decreases, the amplitude of the soliton is enhanced. Figure 7 shows that, as we increase α_2, the grain charge becomes least negative. This causes the grain charge to increase and eventually become positive. In Fig. 8, we show that under certain conditions ($Z_0 = 50$, $f_1 = 3$, $f_2 = 0.2$, $r = 0.1$ μm, $\alpha_1 = 5$, $\alpha_2 = 1$, $\beta = 1/50$, and $n_{d0} = 10^5$ cm^{-3}) the effect of the dust charge variation can be quite important: the nonlinear electrostatic potential, after some spatial oscillatory decaying, levels off at a constant value. The latter represent a collisionless shock wave [62,63] in the sense that no viscous or damping effects resulting from collisions between dust and plasma particles are involved. Thus, the dust charge variation leads to an unusual dissipation of the electrostatic oscillation, which consumes some energy in sustaining the self-consistent dust charge variation. This is a novel feature of dusty plasmas when compared with the ordinary electron–ion plasmas. The energy is given to the current carriers, which drain the charge of the dust grains. This damping is somewhat similar to, but quite distinct from, the nonlinear Landau damping arising from the resonant wave–particle interaction. This process of collisionless power dissipation is of fundamental interest in dusty plasma physics. The spatial profiles of the electron, ion, positron, and dust densities N_e, N_i, N_p, and N_d are given in Fig. 9 (note that $N_i \equiv N_p$ since $\alpha_2 = 1$). The influence of the positrons on the shock front width is displayed in Fig. 10. We note the effect of the charge separation, which is manifested by an appearance of some

https://doi.org/10.1017/S0022377806004636 Published online by Cambridge University Press

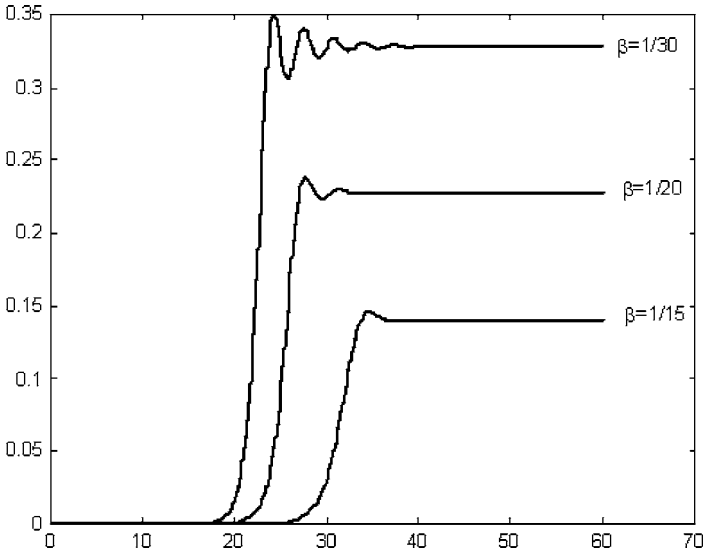


Figure 11. Shock-like solution for the electrostatic potential Ψ for various values of β. The values of the remaining parameters are those used for Fig. 8. The values of $\beta = 1/30$ ($v_{d0} = 278.90$ cm s^{-1}), $1/20$ ($v_{d0} = 227.72$ cm s^{-1}), and $1/15$ ($v_{d0} = 197.21$ cm s^{-1}) are indicated on the figure.

oscillations in the shock wave profile. This effect decreases when the number of positrons increases. Figure 11 indicates that an increase of β (a decrease of $v_{d0} = 278.90$ cm s^{-1}, 227.72 cm s^{-1}, 197.21 cm s^{-1}) gives rise to shocks for which the structure is monotonic instead of being oscillatory as in the case of Fig. 8 ($v_{d0} = 360.07$ cm s^{-1}).

4. Summary

To conclude we have addressed the problem of nonlinear electrostatic solitary waves representing saturated states of a four-stream unstable collisionless charge-varying pair–ion–dust plasma. Our results show that in such a plasma (which is, to our knowledge, yet unexplored and not yet described in the dusty plasma literature) spatially localized structures can exist. Their spatial patterns are significantly modified by the presence of the positron component. In particular, it may be noted that an addition of a small concentration of positrons abruptly reduces the potential pulse amplitude as well as the net negative charge residing on the dust grain surface. The dust density is found to be highly perturbed by the field of the solitary wave. The dust particles are locally expelled and pushed out of the region of the soliton's localization. Furthermore, our results show that the dust charge variation provides an alternate physical mechanism causing dissipation and, as a consequence, causes the wave amplitude to decay and transfer to the so-called noise tail. At present, we do not have any experimental observations of solitary structures in a pair–ion–dust plasma with variable charge to compare with our theoretical predictions. However, considering the wide relevance of nonlinear oscillations in laboratory and space dusty plasmas, our investigation may be taken as a prerequisite for the understanding of the large, but finite-amplitude, solitary waves that may occur

https://doi.org/10.1017/S0022377806004636 Published online by Cambridge University Press

in space and laboratory plasmas. It may be stressed here that the time evolution and stability analysis of these nonlinear plasma structures are problems of great importance but beyond the scope of the present work.

Acknowledgement

This work was supported in part by the Ministère de l'Enseignement Supérieur et de la Recherche Scientifique Contract No. D1602/04/03.

References

[1] Shukla, P. K. 1998 *Proceedings of Invited Papers, 7th Workshop on the Physics of Dusty Plasmas, Boulder, Colorado, April 1998 (Proceedings No. 446)* (ed. M. Horányi, S. Robertson and B. Walch). Woodbury, NY: American Institute of Physics, p. 81.

[2] Rao, N. N. 2000 *Proceedings of Invited Papers, International Workshop on Waves in Dusty, Solar and Space Plasmas, Leuven, Belgium, May 2000* (ed. F. Verheest, M. Goossens, M. A. Hellberg and R. Bharuthram). Melville, NY: American Institute of Physics, vol. 537, p. 13.

[3] Goertz, C. K. 1989 *Rev. Geophys*. **27**, 271.

[4] Mendis, D. A. and Rosenberg, M. 1994 *Ann. Rev. Astron. Astrophys*. **32**, 419.

[5] Horanyi, M. 1996 *Ann. Rev. Astron. Astrophys*. **34**, 383.

[6] Verheest, F. 2000 *Waves in Dusty Space Plasmas*. Dordrecht: Kluwer.

[7] Shukla, P. K. and Mamun, A. A. 2002 *Introduction to Dusty Plasma Physics*. Bristol: Institute of Physics, and references therein.

[8] Verheest, F. 1996 *Space Sci. Rev*. **77**, 267.

[9] Shukla, P. K. 2001 *Phys. Plasmas* **8**, 1447.

[10] Rao, N. N., Shukla, P. K. and Yu, M. Y. 1990 *Planet. Space Sci*. **38**, 543.

[11] Shukla, P. K. and Silin, V. P. 1992 *Phys. Scr*. **45**, 508.

[12] Tribeche, M., Hamdi, R. and Zerguini, T. H. 2000 *Phys. Plasmas* **7**, 4013.

[13] Mamun, A. A., Cairns, R. A. and Shukla, P. K. 1996 *Phys. Plasmas* **3**, 702.

[14] Roychoudhury, R., Venkatesan, S. K. and Das, C. 1997 *Phys. Plasmas* **4**, 4232.

[15] Kotsarenko, N. Ya., Koshevaya, S. V., Stewart, G. A. and Maravilla, D. 1998 *Planet. Space Sci*. **46**, 429.

[16] Sheridan, T. E., Yi, S. and Lonngren, K. E. 1998 *Phys. Plasmas* **5**, 3165.

[17] Mamun, A. A., Alam, M. N. and Azad, A. K. 1998 *Phys. Plasmas* **5**, 1212.

[18] Kakati, M. and Goswami, K. S. 1998 *Phys. Plasmas* **5**, 4508.

[19] Nakamura, Y., Bailung, H. and Lonngren, K. E. 1999 *Phys. Plasmas* **6**, 3466.

[20] Nagasawa, T. 1999 *Phys. Plasmas* **6**, 3471.

[21] Mamun, A. A. 2000 *Eur. Phys. J*. D **11**, 143.

[22] Lontano, M., Bulanov, S. and Koga, J. 2001 *Phys. Plasmas* **8**, 5113.

[23] Esfandyari, A. R., Khorram, S. and Rostami, A. 2001 *Phys. Plasmas* **8**, 4753.

[24] McKenzie, J. F. and Doyle, T. B. 2001 *Phys. Plasmas* **8**, 4367.

[25] Nakamura, Y. and Sarma, A. 2001 *Phys. Plasmas* **8**, 3921.

[26] Ivlev, A. V. and Morfill, G. 2001 *Phys. Rev*. E **63**, 026412-1.

[27] Mamun, A. A., Shukla, P. K. and Stenflo, L. 2002 *Phys. Plasmas* **9**, 1474.

[28] Poornakala, S., Das, A., Sen, A. and Kaw, P. K. 2002 *Phys. Plasmas* **9**, 1820.

[29] Shukla, P. K., Rao, N. N., Yu, M. Y. and Tsintsadze, N. L. 1986 *Phys. Rep*. **135**, 1.

[30] Rizzato, F. B. 1988 *Plasma Phys*. **40**, 289.

[31] Yu, M. Y., Shukla, P. K. and Stenflo, L. 1986 *Astrophys. J*. **309**, L63.

[32] Michel, F. C. 1991 *Theory of Neutron Star Magnetospheres*. Chicago: Chicago University Press.

https://doi.org/10.1017/S0022377806004636 Published online by Cambridge University Press

[33] Tajima, T. and Taniuti, T. 1990 *Phys. Rev.* A **42**, 3587.
[34] Shukla, P. K., Tsintsadze, N. L. and Tsintsadze, L. N. 1993 *Phys. Fluids* B **5**, 811.
[35] Shukla, P. K. 1993 Europhys. Lett. **22**, 695.
[36] Shukla, P. K. and Stenflo, L. 1993 *Astrophys. Space Sci.* **209**, 323.
[37] Tsintsadze, L. N. and Shukla, P. K. 1993 *Plasma Phys. Rep.* **19**, 134.
[38] Berezhiani, V. I., El-Ashry, M. Y. and Mofiz, U. A. 1994 *Phys. Rev.* E **50**, 448.
[39] Tsintsadze, L. N., Tsintsadze, N. L., Shukla, P. K. and Stenflo, L. 1994 *Astrophys. Space Sci.* **222**, 259.
[40] Popel, S. I., Vladimirov, S. V. and Shukla, P. K. 1995 *Phys. Plasmas* **2**, 716.
[41] Kotsarenko, N. Ya., Stewart, G. A. and Vysloukh, V. 1996 *Astrophys. Space Sci.* **243**, 427.
[42] Srinivas, J., Popel, S. I. and Shukla, P. K. 1996 *J. Plasma Phys.* **55**, 209.
[43] Lakhina, G. S. and Verheest, F. 1997 *Astrophys. Space Sci.* **253**, 97.
[44] Mirza, A. M. 2000 *Phys. Plasmas* **7**, 3588.
[45] Haque, Q., Saleem, H. and Vranjes, J. 2002 *Phys. Plasmas* **9**, 474.
[46] Saleem, H., Haque, Q. and Vranjes, J. 2003 *Phys. Rev.* E **67**, 057402.
[47] Verga, A. D. and Ferro Fontán, C. 1984 *Phys. Lett.* A **101**, 494.
[48] da Costa, A. A., Diver, D. A. and Stewart, G. A. 2001 *Astron. Astrophys.* **366**, 129.
[49] Rizzato, F. B. 1998 *J. Plasma Phys.* **40**, 289.
[50] Shukla, P. K., Farid, T., Stenflo, L. and Onishchenko, O. G. 2000 *J. Plasma Phys.* **64**, 427.
[51] Mirza, A. M., Farid, T., Shukla, P. K. and Stenflo, L. 2001 *IEEE Trans. Plasma Sci.* **29**, 298.
[52] Cho, S. H., Lee, H. J. and Kim, Y. S. 2000 *Phys. Rev.* E **61**, 4357.
[53] Shukla, P. K. and Marklund, M. 2004 *Phys. Scr.* **T113**, 36.
[54] Shin, D. S. and Jung, Y. D. 2006 *Phys. Lett.* A **349**, 500.
[55] Tribeche, M., Zerguini, T. H. and Houili, H. 2002 *Phys. Plasmas* **9**, 4879.
[56] Chen, F. F. 1965 *Plasma Diagnostic Techniques* (ed. R. H. Huddlestone and S. L. Leonard). New York: Academic Press, ch. 4.
[57] Barnes, M. S., Keller, J. H., Forster, J. C., O'Neill, J. A. and Coultas, D. K. 1992 *Phys. Rev. Lett.* **68**, 313.
[58] Ma, J. X. and Yu, M. Y. 1995 *Phys. Plasmas* **2**, 1343.
[59] Whipple, E. C. 1981 *Rep. Prog. Phys.* **44**, 1198.
[60] Ma, J. X., Liu, J.-y. and Yu, M. Y. 1997 *Phys. Rev.* E **55**, 4627.
[61] Liu, J.-y. and Ma, J. X. 1997 *Phys. Plasmas* **4**, 2798.
[62] Gupta, M. R., Sarkar, S., Ghosh, S., Debnath, M. and Khan, M. 2001 *Phys. Rev.* E **63**, 046406-1.
[63] Popel, S. I., Yu, M. Y. and Tsytovich, V. N. 1996 *Phys. Plasmas* **3**, 4313.

https://doi.org/10.1017/S0022377806004636 Published online by Cambridge University Press